Postprint (accepted version)
The final publication is available at http://ieeexplore.ieee.org/xpl/articleDetails.jsp?arnumber=6255761
DOI: 10.1109/LSP.2012.2210873

S. Sugiura, A. Ichiki, and Y. Tadokoro, "Stochastic-resonance based iterative detection for serially-concatenated turbo codes," IEEE Signal Processing Letters, vol. 19, no. 10, pp. 655-658, Oct. 2012.

© 2012 IEEE. Personal use of this material is permitted. Permission from IEEE must be obtained for all other uses, in any current or future media, including reprinting/republishing this material for advertising or promotional purposes, creating new collective works, for resale or redistribution to servers or lists, or reuse of any copyrighted component of this work in other works

Stochastic-Resonance Based Iterative Detection for Serially-Concatenated Turbo Codes

Shinya Sugiura, *Senior Member, IEEE*, Akihisa Ichiki, and Yukihiro Tadokoro, *Member, IEEE*

***Abstract*—In this letter, the concept of multiple serially-concatenated codes is invoked in the context of stochastic resonance (SR), where the achievable performance is improved by increasing noise power. More specifically, the receiver's iterative decoding process is characterized with the aid of extrinsic information transfer (EXIT) charts, such that the SR effect induced by a non-linear component is taken into account. Our simulation results demonstrate that although the SR demodulator's log-likelihood ratio (LLR) outputs are not Gaussian distributed, the corresponding EXIT trajectory matches the prediction from the associated inner- and outer-codes' EXIT curves, while reaching the perfect convergence point in terms of mutual information. Therefore, an infinitesimally low bit-error ratio (BER) is attained by appropriately designing the channel code's parameters based on EXIT charts.**

***Index Terms*—Comparator, EXIT chart, non-linear systems, irregular codes, iterative detection, stochastic resonance.**

I. Introduction

STOCHASTIC resonance (SR) is a physical phenomenon, which has the potential of improving the receiver's detection performance, upon increasing the power of the additive noise contaminating the signal. Typically, such an SR effect can be observed in non-linear (NL) systems [1]–[3]. For these reasons, the SR is especially useful in a scenario, where a small signal is corrupted by additive noise and the NL effects imposed by the receiver are intrinsically unavoidable. However, owing to the presence of a NL component, it is a challenging task to theoretically characterize its achievable performance. The seminal studies [1], [2] focused on the signal-to-noise ratio (SNR) metric in order to evaluate the SR effect in a relatively simple manner. Furthermore, in [4], [5] it was also found that SR improves the mutual information (MI) exchange between the input and output signals. Considering that the specific definition of SNR depends on the SR scenarios considered and that as mentioned in [3], the SNR is not directly related to the achievable detection performance, especially for non-Gaussian noise scenarios, it can be said that the MI is a more suitable performance metric for the scenario considered. Note that in order to practically attain a near-capacity performance, which may be characterized by near-unity MI, it is necessary to incorporate a channel code into the system.

On the other hand, to the best of our knowledge, the previous SR related studies [6]–[10] only considered uncoded scenarios. However, practical systems typically employ a powerful channel coding scheme, such as turbo [11] and low-density parity-check (LDPC) codes [12], which are capable of increasing MI between the input/output signals, upon iterating between multiple soft decoders. Furthermore, in [13] the semi-analytical tool of extrinsic information transfer (EXIT) charts was proposed for the sake of accurately predicting the convergence behavior of the iterative decoding process, which allows us to optimize multiple concatenated codes.

Against this background, the novel contributions of this letter are as follows. We first propose a channel-encoded SR system, which is capable of attaining a near-capacity performance. More specifically, a serially-concatenated turbo code, employing the NL component of a single-comparator, is optimized with the aid of EXIT charts. Furthermore, we prove that an infinitesimally low bit error ratio (BER) is achievable by appropriately designing the channel code as well as by providing a sufficient number of iterations amongst multiple decoders. Another important finding is that our EXIT-chart aided convergence prediction is also useful even in the scenario, where the system includes a NL component as well as additive non-Gaussian noise.

II. System Description

A. System Model

Consider the transmitter structure of Fig. 1, supporting multiple serially-concatenated codes, namely a channel encoder and a precoder. At the transmitter, B information bits b_i $(i = 1, \cdots, B)$ are firstly channel encoded by a convolutional encoder, having a code rate of $R_{\rm CC}$. The $C = B/R_{\rm CC}$ channel-encoded bits c_i $(i = 1, \cdots, C)$ are then interleaved by a random interleaver Π. Furthermore, the interleaved bits are encoded by a unity-rate convolutional (URC) code[1]. The coded bits are finally mapped to binary phase-shift keying (BPSK) symbols $s_i \in \{+1, -1\}$ $(i = 1, \cdots, C)$, which are transmitted to the receiver over additive noisy channels.

At the receiver, N signals $r_i^{(n)}$ $(n = 1, \cdots, N)$ are sampled per transmitted symbol s_i, which are represented by

$$r_i^{(n)} = s_i + \eta_i^{(n)}. \tag{1}$$

More specifically, we assume that the real-valued additive noise $\eta_i^{(n)}$ is an identically and independently distributed (IID) variable, which obeys the Gaussian-mixture distribution having the probability density function (PDF) of [7]

$$f(u,\sigma) = \frac{1}{2\sigma\sqrt{2\pi(1-\beta^2)}} \times \left\{ \exp\left[-\frac{(u/\sigma+\beta)^2}{2(1-\beta^2)} \right] + \exp\left[-\frac{(u/\sigma-\beta)^2}{2(1-\beta^2)} \right] \right\}, \tag{2}$$

Copyright (c) 2012 IEEE. Personal use of this material is permitted. However, permission to use this material for any other purposes must be obtained from the IEEE by sending a request to pubs-permissions@ieee.org.

The authors are with Toyota Central R&D Laboratories, Inc., Nagakute, Aichi, 480-1192, Japan (e-mail: sugiura@ieee.org).

[1]The role of the URC code is to impose an infinite impulse response (IIR), which improves the achievable iterative decoding performance by efficiently spreading the extrinsic information, as detailed in [14].

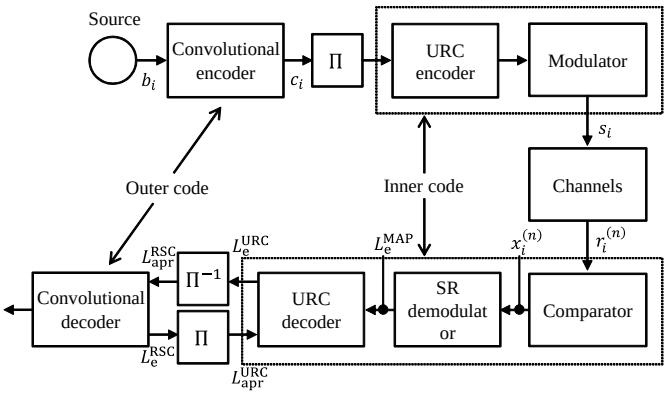

Fig. 1. The iteratively-detected transceiver structure of our RSC-coded and unity-rate precoded SR system, employing a single comparator.

where σ represents the standard deviation, while the value of β is in the range of $0 < \beta < 1$[2]. Here, as β approaches zero, $f(u,\sigma)$ becomes similar to the zero-mean unit-variance Gaussian distribution. Moreover, the corresponding cumulative distribution function (CDF) can be formulated by

$$F(u,\sigma) = \frac{1}{2} + \frac{1}{4}\left[\mathrm{erf}\left(\frac{u/\sigma+\beta}{\sqrt{2(1-\beta^2)}}\right) + \mathrm{erf}\left(\frac{u/\sigma-\beta}{\sqrt{2(1-\beta^2)}}\right)\right]. \quad (3)$$

Then, the sampled signals $r_i^{(n)}$ are passed onto the comparator of Fig. 1, which has a threshold of θ. The comparator's outputs $\mathbf{x}_i = \left[x_i^{(1)}, \cdots, x_i^{(N)}\right]$ are as follows:[3]

$$x_i^{(n)} = \begin{cases} 1 & (r_i^{(n)} \geq \theta) \\ 0 & (r_i^{(n)} < \theta) \end{cases}. \quad (4)$$

Next, the binary sequence $\mathbf{x}_i$ is input to the soft-input soft-output (SISO) SR demodulator of Fig. 1, where the extrinsic information $L_{\rm e}$ expressed in the form of log-likelihood ratios (LLRs) is calculated under the assumption of perfect knowledge of the standard deviation σ. Although there are several algorithms, which may be employed by the SISO detector, in this letter we adopt optimal maximum *a posteriori* (MAP) detection, which is described later in Section II-B.

Assuming that in this letter a recursive systematic convolutional (RSC) code is used for the convolutional encoder/decoder of Fig. 1, the receiver employs iterative detection between the two SISO decoders [11], [16], i.e. the URC and RSC decoders[4]. To be more specific, the URC decoder outputs the extrinsic information $L_{\rm e}^{\rm URC}$ in the form of LLRs with the aid of the SISO MAP detector's outputs $L_{\rm e}^{\rm MAP}$ as well as of the *a priori* LLRs $L_{\rm apr}^{\rm URC}$, which are fed back from the convolutional decoder to the URC decoder. The extrinsic LLRs $L_{\rm e}^{\rm URC}$ are then input to the RSC decoder after deinterleaving. The extrinsic LLRs $L_{\rm e}^{\rm RSC}$ are calculated at the RSC decoder, output and are interleaved again, before being passed back to the SISO URC decoder as the *a priori* information $L_{\rm apr}^{\rm URC}$. Finally, the RSC decoder outputs the estimated bits $\hat{b}_i$ after I number of iterations. We note that since there is no *a priori* information during the first iteration, the initial values of $L_{\rm apr}^{\rm URC}$ are set to zero.

B. The Optimal MAP Detector

Let us now derive the *a posteriori* LLR $L_{\rm apo}^{\rm MAP}$, which is calculated based on the optimal MAP criterion as follows:

$$L_{\rm apo}^{\rm MAP} = \ln\left[\frac{p(\mathbf{x}_i|s_i=-1)P_1}{p(\mathbf{x}_i|s_i=+1)P_0}\right] \quad (5)$$

$$= \underbrace{\ln\left(\frac{P_1}{P_0}\right)}_{L_{\rm apr}^{\rm MAP}} + \underbrace{\ln\left[\frac{\prod_{n=1}^{N} p(x_i^{(n)}|s_i=-1)}{\prod_{n=1}^{N} p(x_i^{(n)}|s_i=+1)}\right]}_{L_{\rm e}^{\rm MAP}}, \quad (6)$$

where $L_{\rm apr}^{\rm MAP}$ and $L_{\rm e}^{\rm MAP}$ represent the *a priori* and extrinsic LLRs, while P_0 and P_1 are the *a priori* probabilities, which correspond to the events of $s_i = -1$ and 1, respectively.

Since the comparator's output is binary, its conditional probability density may be expressed as

$$p(x_i^{(n)}|s_i) = \begin{cases} F(\theta - s_i, \sigma) & (x_i^{(n)} = 0) \\ 1 - F(\theta - s_i, \sigma) & (x_i^{(n)} = 1) \end{cases}. \quad (7)$$

Considering that the possible number of non-zero elements, which are contained in the comparator's binary outputs $\mathbf{x}_i$, is varied from 0 to N, the legitimate number of the potential extrinsic LLRs $L_{\rm e}^{\rm MAP}$ is equal to $(N+1)$, given the specific system parameters of (N, σ, θ). This implies that the related *a priori* LLR values, which are input from the SR MAP detector to the URC decoder, are not Gaussian distributed in the comparator-based scenario of Fig. 1. Nevertheless, we will show later in Section III that the corresponding EXIT trajectory matches the inner- and outer-EXIT curves, as expected for a Gaussian scenario.

C. EXIT-Chart Analysis

In this section, we briefly highlight the concept of EXIT charts, which is a powerful technique used for analyzing the convergence behavior of iterative detection aided transmissions based on the turbo-coding principle. For further detailed

[2]Note that additive Gaussian mixture noise has been widely adopted in the diverse SR-related studies [3], [7]–[9]. More specifically, one of its explicit examples is constituted by multiuser interference and impulsive noise in code-division multiple access (CDMA) systems [15], while this Gaussian-mixture framework may also be applicable to several other impulsive electromagnetic interference scenarios, such as automobile ignition noise, military mobile channels and indoor interference induced by mechanical switching.

[3]In order to expound a little further, we employed a comparator as a NL component. However, other NL effects, such as particular NL channels and bistable-potential systems [10], can be readily applicable to our proposed architecture.

[4]Since in this letter the SISO MAP detector calculates extrinsic information $L_{\rm e}^{\rm MAP}$ based on a binary input sequence x_i^n, it remains unaffected by the potential feedback from the URC decoder, which is referred to as $L_{\rm apr}^{\rm MAP}$. On the other hand, when employing multi-level constellations are input to the MAP detector instead of x_i^n, its extrinsic LLR values $L_{\rm e}^{\rm MAP}$ also become affected by $L_{\rm apr}^{\rm MAP}$. In such a scenario, iterations between the SISO MAP detector and the SISO URC decoder further improve the achievable performance, as mentioned in [11].

explanations of EXIT charts, refer to [16] and the references therein. In turbo detection, an infinitesimally low BER may be attained by the iterative exchange of extrinsic MI between two SISO decoders, i.e. the inner and outer decoders. Since the iterative decoding process is not linear, the prediction of its convergence behavior is a challenging task.

The ingenious tool of EXIT charts was proposed by ten Brink [13] for the visualization of the iterative decoding behavior and for the prediction of the 'BER-cliff' position, where the BER suddenly drops. More specifically, the input/output relationship of the MI at each decoder is characterized by the EXIT chart and then their interaction assisted by the iterative decoding process is examined without time-consuming bit-by-bit Monte-Carlo simulations. Ideally, the inner and outer decoders' EXIT curves should not intersect before the perfect convergence point of $(I_{\rm A}, I_{\rm E}) = (1.0, 1.0)$, which leads to perfect extrinsic information exchange between the two decoders of Fig. 1. The emergence of an open EXIT chart convergence tunnel enables the system to achieve an infinitesimally low BER at the corresponding SNR.

Furthermore, the maximum achievable rate may be formulated based on the inner code's EXIT curve as follows: [16]

$$R = R_{\rm CC}\mathcal{A} \cdot \log_2 \mathcal{M} \quad [\text{bits/symbol}], \tag{8}$$

where $0 \leq R_{\rm CC} \leq 1$ represents the RSC code's rate and $0 \leq \mathcal{A} \leq 1$ denotes the area under the inner decoder's EXIT curve [16]. Moreover, $\mathcal{M}$ is the number of constellation points, which is fixed to $\mathcal{M} = 2$ in this letter. We note that the maximum achievable rate of Eq. (8) may be useful for the SR-aided systems, since the corresponding inner decoder's EXIT curve takes into account the effects of NL components.

III. Simulation Results

In this section, we provide our performance results in order to characterize the proposed RSC-coded and unity-rate precoded SR scheme in the context of the single-comparator-based NL system.

We assumed that the number of information bits per frame was $B = 10^5$, while considering the three different half-rate RSC codes, namely the length-two RSC(2,1,2) code, the length-three RSC(2,1,3) code and the length-five RSC(2,1,5) code, having the octal generator polynomials of $(G_r, G) = (3, 2)_8$, $(G_r, G) = (7, 5)_8$ and $(G_r, G) = (35, 23)_8$, respectively. The threshold value of the receiver's comparator was set to $\theta = 1.5$[5]. Furthermore, the Gaussian-mixture noise process was characterized by $\beta = 0.9$. Additionally, the information bits b_i were equi-probably distributed.

Firstly, Fig. 2 shows the maximum achievable rates of our arrangements, which were obtained according to Eq. (8). Here, the number of samples per symbol was varied from $N = 1$ to 5. Observe in Fig. 2 that upon increasing the standard deviation σ from zero to approximately $\sigma = 1.1$, the maximum achievable rate monotonically increased in each scenario, which is achieved as the explicit merit of SR. To be more specific, this SR effect is especially beneficial for low-SNR scenarios, albeit this is achieved by sacrificing the achievable performance in the low-noise regime, as shown in Fig. 2. By contrast, in the high-noise range of $\sigma > 1.1$, an increase in the value of σ degraded the achievable performance, in a similar manner to its linear-system counterpart. Furthermore, as expected, a higher number of samples N leads to a higher maximum achievable rate, which is a benefit of having a higher sampling frequency. In order to provide further insights, since a half-rate ($R_{\rm CC} = 0.5$) channel code was employed in our simulations, the scenarios of $N = 3, 4$ and 5 have the potential of attaining a near-error-free performance around the noise root-mean-square (RMS) value of $\sigma = 1$, as shown in Fig. 2.

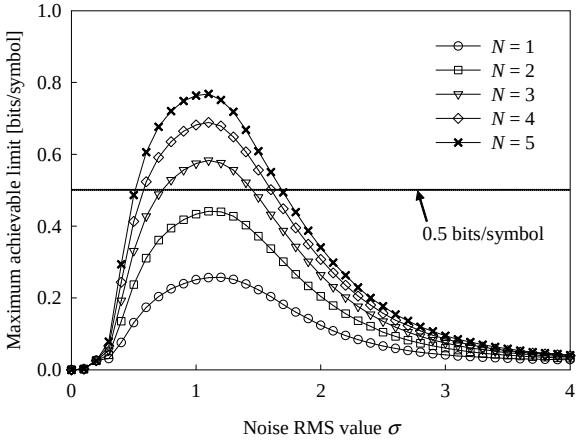

Fig. 2. The maximum achievable rates of our RSC-coded and URC-precoded SR system, employing a single comparator. Here, the number of samples per symbol was varied from $N = 1$ to 5.

Furthermore, the inner- and outer-codes' EXIT curves were drawn in Fig. 3, where we varied the standard deviation from $\sigma = 0.7$ to 1.3 with the step of 0.2, while the number of samples per symbol was $N = 3$. Furthermore, we plotted the outer code's EXIT curves, which correspond to the three aforementioned half-rate RSC codes, as well as to the EXIT trajectory associated with $\sigma = 1.1$ and the RSC(2,1,2) code. It was found from Fig. 3 that an open tunnel emerged between the inner- and outer-codes' EXIT curves for the scenario of $\sigma = 1.1$ and the RSC(2,1,2) code. More specifically, the EXIT trajectory of $\sigma = 1.1$ reached the perfect convergence point of $(I_{\rm A}, I_{\rm E}) = (1, 1)$, while reasonably matching the corresponding inner- and outer-codes' EXIT curves.[6]

Finally, Fig. 4 compares the achievable BER of the channel coded system corresponding to the trajectory of Fig. 3, where the number of iterations I was given by $I = 0, 5, 10, 20$ and 35. As predicted from the EXIT charts of Fig. 3, a near-error-free performance was achieved around $\sigma = 1.1$ with the aid

[5]Here, the thresholding value θ was determined from our extensive simulations, though it does not guarantee its optimality. The related investigation is an open issue.

[6]The application of EXIT chart is based on the assumption that the *a priori* LLR values are uncorrelated and that their PDF is Gaussian distributed [16]. Our SR-based turbo-coded system of Fig. 1 does not apply to this, since the legitimate number of the MAP detector's extrinsic LLR values $L_{\rm e}^{\rm MAP}$ is $(N+1)$. However, Fig. 3 shows that the effects of the non-Gaussian distributed *a priori* LLR are not severe in the simulated scenarios, which still enables us to predict the convergence behavior of the iterative process.

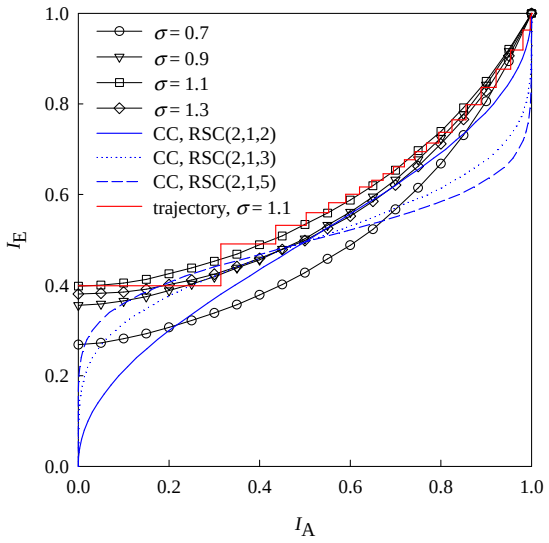

Fig. 3. EXIT charts of our RSC-coded and URC-precoded SR system, employing a single comparator. Here, the standard deviation of Gaussian-mixture noise was varied from $\sigma = 0.7$ to 1.3 with the step of 0.2, while the number of samples per symbol was $N = 3$. Furthermore, the outer EXIT curve of half-rate length-two RSC(2,1,2), length-three RSC(2,1,3) and length-five RSC(2,1,5) codes were considered. We also plotted the EXIT trajectory, which was associated with $\sigma = 1.1$, the interleaver length of $C = 2 \times 10^5$ and the RSC(2,1,2) code.

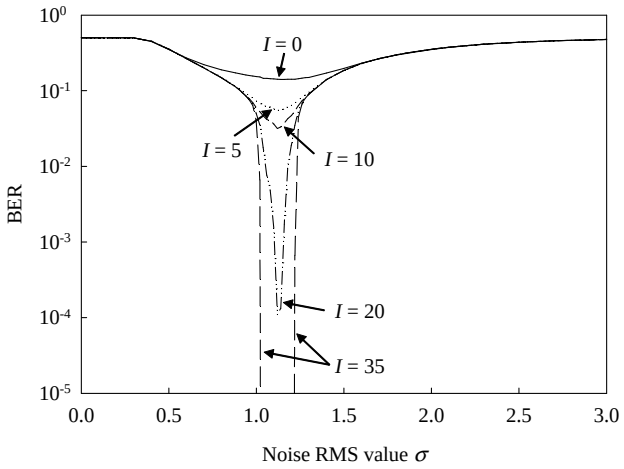

Fig. 4. Achievable BER performance of our RSC-coded and URC-precoded SR system, employing a single comparator. The number of iterations was given by $I = 0, 5, 10, 20$ and 35, while the number of samples per symbol was maintained to be $N = 3$.

of a sufficiently high number of iterations I. Additionally, it is specific to the SR scheme of Fig. 1 that a so-called 'BER cliff' [16] was found not only for a low σ but also for a high σ, which is not observed in the classic-modem scenarios.

An important implication of the above-mentioned simulation results is that by adaptively matching the shape of the outer code's EXIT curve to that of the inner code with the aid of irregular channel coding [16], an infinitesimally low BER may be achieved over a wide range of SNRs.

In this letter, we focused our attention on the scenario of using a single comparator [6], which acts as a 1-bit quantizer. However, the proposed system can be readily extended to other nonlinear systems, such as a multiple-comparator based one [17], which may further improve the SR performance, although the detailed investigations will be left for our future study.

IV. Conclusions

In this letter, we proposed the serially-concatenated channel-encoded arrangement of Fig. 1 in the context of SR. More specifically, the concept of EXIT charts was invoked for analyzing the convergence behavior of iterative decoding process, while taking into consideration the effects of the NL component and the non-Gaussian noise. Our simulation results showed that an infinitesimally low BER performance is achievable in our arrangement, as predicted from the associated EXIT charts. It was also implied that an adaptive channel coding scheme based on the irregular code may be useful for SR-aided NL systems, similarly to its linear-system counterpart [16].

References

[1] P. Jung and P. Hänggi, "Amplification of small signals via stochastic resonance," *Physical Review A*, vol. 44, no. 12, pp. 8032–8042, 1991.
[2] J. Collins, C. Chow, and T. Imhoff, "Stochastic resonance without tuning," *Nature*, vol. 376, no. 20, pp. 236–238, 1995.
[3] H. Chen, P. Varshney, S. Kay, and J. Michels, "Theory of the stochastic resonance effect in signal detection: Part I - fixed detectors," *IEEE Transactions on Signal Processing*, vol. 55, no. 7, pp. 3172–3184, 2007.
[4] I. Goychuk and P. Hänggi, "Stochastic resonance in ion channels characterized by information theory," *Physical Review E*, vol. 61, no. 4, pp. 4272–4280, 2000.
[5] S. Mitaim and B. Kosko, "Adaptive stochastic resonance in noisy neurons based on mutual information," *IEEE Transactions on Neural Networks*, vol. 15, no. 6, pp. 1526–1540, 2004.
[6] F. Chapeau-Blondeau, "Nonlinear test statistic to improve signal detection in non-Gaussian noise," *IEEE Signal Processing Letters*, vol. 7, no. 7, pp. 205 –207, July 2000.
[7] S. Zozor and P. Amblard, "On the use of stochastic resonance in sine detection," *Signal Processing*, vol. 82, no. 3, pp. 353–367, 2002.
[8] ——, "Stochastic resonance in locally optimal detectors," *IEEE Transactions on Signal Processing*, vol. 51, no. 12, pp. 3177–3181, 2003.
[9] F. Chapeau-Blondeau and D. Rousseau, "Raising the noise to improve performance in optimal processing," *Journal of Statistical Mechanics: Theory and Experiment*, vol. 2009, p. P01003, 2009.
[10] A. Ichiki, Y. Tadokoro, and M. I. Dykman, "Singular response of bistable systems driven by telegraph noise," *Physical Review E*, vol. 85, p. 031106, Mar. 2012.
[11] S. Sugiura, S. Chen, and L. Hanzo, "MIMO-aided near-capacity turbo transceivers: Taxonomy and performance versus complexity," *IEEE Communications Surveys & Tutorials*, vol. 14, no. 2, pp. 421–442, Second Quarter 2012.
[12] T. Richardson and R. Urbanke, *Modern coding theory*. Cambridge University Press, 2008.
[13] S. ten Brink, "Convergence behavior of iteratively decoded parallel concatenated codes," *IEEE Transactions on Communications*, vol. 49, no. 10, pp. 1727–1737, 2001.
[14] D. Divsalar, S. Dolinar, and F. Pollara, "Serial concatenated trellis coded modulation with rate-1 inner code," in *IEEE Global Telecommunications Conference*, vol. 2, San Francisco, CA, November–December 2000, pp. 777–782.
[15] X. Wang and H. Poor, "Robust multiuser detection in non-Gaussian channels," *IEEE Transactions on Signal Processing*, vol. 47, no. 2, pp. 289–305, 1999.
[16] L. Hanzo, O. Alamri, M. El-Hajjar, and N. Wu, *Near-Capacity Multi-Functional MIMO Systems: Sphere-Packing, Iterative Detection and Cooperation*. John Wiley and IEEE Press, 2009.
[17] N. Stocks, "Suprathreshold stochastic resonance in multilevel threshold systems," *Physical Review Letters*, vol. 84, no. 11, pp. 2310–2313, 2000.